Available online at www.sciencedirect.com
ScienceDirect
Journal of Solid State Chemistry 180 (2007) 596–603
JOURNAL OF SOLID STATE CHEMISTRY
www.elsevier.com/locate/jssc

Preparation, crystal structure and thermal expansion of a new bismuth barium borate, $BaBi_2B_4O_{10}$

R.S. Bubnova[a], S.V. Krivovichev[b], S.K. Filatov[b,*], A.V. Egorysheva[c], Y.F. Kargin[c]

[a]*Grebenshchikov Institute of the Silicate Chemistry of the Russian Academy of Sciences, Makarov Emb. 2, St. Petersburg 199034, Russian Federation*
[b]*Department of Crystallography, St. Petersburg State University, University Emb. 7/9, 199034 St. Petersburg, Russian Federation*
[c]*Kurnakov Institute of General and Inorganic Chemistry of the Russian Academy of Sciences, Leninsky Prospect 31, GSP-1, Moscow 119991, Russian Federation*

Received 26 September 2006; received in revised form 1 November 2006; accepted 4 November 2006
Available online 9 November 2006

Abstract

Single crystals of a new compound, $BaBi_2B_4O_{10}$ were grown by cooling a melt with the stoichiometric composition. The crystal structure of the compound has been solved by direct methods and refined to $R_1 = 0.049$ ($wR = 0.113$) on the basis of 1813 unique observed reflections ($|F_o| > 4\sigma|F_o|$). It is monoclinic, space group $P2_1/c$, $a = 10.150(2)$, $b = 6.\ 362(1)$, $c = 12.485(2)$ Å, $\beta = 102.87(1)^o$, $V = 786.0(2)$ Å^3, $Z = 4$. The structure is based upon anionic thick layers that are parallel to (001). The layers can be described as built from alternating novel borate $[B_4O_{10}]^{8-}_{\infty}$ chains and bismuthate $[Bi_2O_5]^{4-}_{\infty}$ chains extended along *b*-axis. The borate chains are composed of $[B_3O_8]^{7-}$ triborate groups of three tetrahedra and single triangles with a $[BO_2]^-$ radical. The borate chains are interleaved along the *c*-axis with rows of the Ba^{2+} cations so that the Ba atoms are located within the layers. The layers are connected by two nonequivalent Ba–O bonds as well as by two equivalent Bi–O bonds with bond valences in the range of 0.2–0.3 v.u.

Thermal expansion of $BaBi_2B_4O_{10}$ studied by high-temperature X-ray powder diffraction in the temperature range of 20–700 °C (temperature step 30–35 °C) is highly anisotropic. While the *b* and *c* unit-cell parameters increase almost linearly on heating, temperature dependencies of *a* parameter and β monoclinic angle show nonlinear behavior. As a result, on heating orientation of thermal expansion tensor changes, and bulk thermal expansion increases from $20 \times 10^{-6}\,°C^{-1}$ at the first heating stage up to $57 \times 10^{-6}\,°C^{-1}$ at 700 °C that can be attributed to the increase of thermal mobility of heavy Bi^{3+} and Ba^{2+} cations.

Keywords: Barium bismuth borate; Crystal structure determination; Thermal expansion

1. Introduction

Nowadays borates have received great attention of material scientists due to their interesting nonlinear optical [1–5], piezoelectric [6], luminescent and other useful properties [7,8] for technical applications. Unique character of crystal structures of borates determines their enhanced UV transparency, good nonlinearity and relatively high resistance against laser-induced damage. Recently theoretical calculations [9,10] showed that NLO properties of α-BiB_3O_6 are due to BiO_4^{5-} anionic groups and not only due to borate groups as is the case for other borates. This induced a considerable interest in search for new promising compounds for non-linear optics in ternary borate systems such as Bi_2O_3–R_xO_y–B_2O_3 where $R = Na^+$ [11], K^+ [12], Ba^{2+} [13–15], Al^{3+} [16] and others.

The Bi_2O_3–BaO–B_2O_3 ternary system is of special interest since it includes, among other compounds, well-known NLO compound, β-BaB_2O_4 [17,18], and highly promising material BiB_3O_6 [19–21]. Crystal structures for most of the homometallic compounds in this system have already been reported. The Bi compounds studied are $Bi_{24}B_2O_{39}$ [22], $Bi_4B_2O_9$ [23], $Bi_3B_5O_{12}$ [24,25], $BiBO_3$ [26], α- [27], β- and γ-BiB_3O_6 [28], and $Bi_2B_8O_{15}$ [29,30]. In the BaO–B_2O_3 system, structures have been reported for $Ba_5(BO_3)_2(B_2O_5)$ [31], α- [32] and β-BaB_2O_4 [33], BaB_4O_7 [34], $Ba_2B_{10}O_{17}$ [35] and BaB_8O_{13} [36]. However, only a few

*Corresponding author.
E-mail address: filatov@crystal.pu.ru (S.K. Filatov).

0022-4596/$ - see front matter © 2006 Elsevier Inc. All rights reserved.
doi:10.1016/j.jssc.2006.11.001

ternary borate compounds are known in the system [13,15]. Recently Barbier et al. [13] reported synthesis and NLO properties a novel noncentrosymmetric barium bismuth borate, $BaBiBO_4$, and reported its crystal structure. The NLO properties of this compound have been explained as a result of the presence in the crystal structure of both borate and bismuthate groups [13]. Here we report synthesis, crystal structure and thermal expansion of $BaBi_2B_4O_{10}$, another new compound discovered in the $BaO–Bi_2O_3–B_2O_3$ system [14].

2. Experimental

2.1. Synthesis

Single crystals of $BaBi_2B_4O_{10}$ were obtained by cooling down a melt with the stoichiometric composition. First, the starting charge consisting of Bi_2O_3, $BaCO_3$ and H_3BO_3 (high purity grade) was sintered by a solid-state reaction in closed platinum crucibles within electric furnace at 600 °C. Then the mixture was heated to 750 °C that is higher than the melting temperature of the compound (730 °C [14,15]). After that the sample was cooled down with the rate of 0.5°/h.

2.2. Crystal-structure determination

The crystal selected for data collection was examined under an optical microscope and mounted on a glass fiber. Data were collected by means of a STOE IPDS II diffractometer using monochromated MoKα radiation and framewidths of 2° in ω. The unit-cell dimensions (Table 1) were refined by least-squares techniques. The data were corrected for Lorentz, polarization, absorption, and background effects. The intensity statistics indicated the centrosymmetric space group $P2_1/c$. The structure was solved and refined by means of the programs SIR-92 [37] and SHELXL-97 [38], respectively. The final models included anisotropic displacement parameters for cations only. Attempts to refine anisotropic parameters of O positions resulted in physically unrealistic values. The final atomic positional and displacement parameters are given in Table 2. Selected interatomic distances are in Table 3. Tables of anisotropic displacement parameters for the Ba and Bi^{3+} atoms, and calculated and observed structure factors have been sent to the Fachinformationzentrum Karlsruhe, Abt. PROKA, 76344 Eggenstein-Leopoldshafen, Germany as supplementary material No. SUP 417181 and can be obtained by contacting the FIZ (quoting the article details and the corresponding SUP number).

2.3. High-temperature X-ray powder diffraction study

Thermal expansion of $BaBi_2B_4O_{10}$ was studied in air using in situ high-temperature X-ray powder diffraction data collected by means of the DRON-3 X-ray diffractometer with a high-temperature KRV-1100 camera, Cu$K\alpha$-radiation. The sample was prepared from heptane's suspension on a Pt plate. The temperature steps were 30–35 °C, average heating rate was about 1–2 °C/min in the range of 20–700 °C. Unit cell parameters of the compound at different temperatures were refined by the least-square methods. Main coefficients of the thermal expansion tensor including its orientation relatively crystallographic axes were determined using polynomial approximation of temperature dependencies for the unit-cell parameters in the range of 20–700 °C by Belousov and Filatov program [39].

Table 1
Crystallographic data and refinement parameters for $BaBi_2B_4O_{10}$

a (Å)	10.150 (2)
b (Å)	6.362(1)
c (Å)	12.485(2)
β (°)	102.87 (1)
V (Å^3)	786.0(2)
Space group	$P2_1/c$
μ (mm^{-1})	49.671
Z	4
D_{calc} (g/cm^3)	6.410
Crystal size (mm^3)	$0.14 \times 0.08 \times 0.06$
Diffractometer	Stoe IPDS II
Radiation	Mo$K\alpha$
Total Ref.	6949
Unique Ref.	2109
2θ range, °	4.12–58.26
Unique $\lvert F_o\rvert \leqslant 4\sigma_F$	1813
R_{int}	0.057
R_σ	0.054
R_1	0.049
wR_2	0.113
S	1.144

Note: $R_1 = \Sigma||F_o|-|F_c||/\Sigma|F_o|$; $wR2 = \{\Sigma[w(F_o^2-F_c^2)^2]/\Sigma[w(F_o^2)^2]\}^{1/2}$; $w = 1/[\sigma^2(F_o^2) + (aP)^2 + bP]$, where $P = (F_o^2 + 2F_c^2)/3$; $s = \{\Sigma[w(F_o^2-F_c^2)]/(n-p)\}^{1/2}$ where n is the number of reflections and p is the number of refined parameters.

3. Results and discussion

3.1. Crystal structure

3.1.1. Cation and anion coordination

There are four symmetrically independent B atoms in the structure of $BaBi_2B_4O_{10}$ (Fig. 1). The B(2) atom is coordinated by three O atoms in a triangular arrangement, whereas the B(1), B(3) and B(4) atoms are tetrahedrally coordinated by four O atoms each. The B–O bonds in the BO_3 triangles are in the range of 1.36–1.40 Å, and the average $\langle {}^{III}B–O \rangle$ bond length for triangle in the structure is 1.375 Å. The B–O bond lengths in the BO_4 tetrahedra vary from 1.43 to 1.56 Å, with an average $\langle {}^{IV}B–O \rangle$ bond length for tetrahedra of 1.481 Å. The O–B–O angles range from 117° to 122° for a BO_3 triangle and from 103° to 113° for BO_4 tetrahedra. The average bond lengths for both polyhedra as well as ranges of individual B–O bond lengths and O–B–O angles are in good agreement with those reported in [40].

Table 2
Atomic coordinates, displacement parameters (Å^2) and bond valence sums (BVS, v.u.) for $BaBi_2B_4O_{10}$

Atom	x/a	y/b	z/c	U_{iso}	BVS[a]	BVS[b]
Bi(1)	0.48513(5)	0.17579(8)	0.11842(4)	0.00379(17)	3.21	3.00
Bi(2)	0.72720(5)	0.14836(9)	0.37226(4)	0.00397(17)	3.05	2.86
Ba	0.12784(9)	0.09472(14)	−0.12314(7)	0.0047(2)	2.30	2.30
O(1)	0.3127(11)	0.4358(18)	−0.1120(9)	0.007[c]	1.84	1.84
O(2)	0.7122(10)	−0.2137(17)	0.2754(8)	0.0035(18)	2.08	2.18
O(3)	0.5628(11)	−0.1254(18)	0.0959(9)	0.006(2)	2.08	1.94
O(4)	−0.1307(10)	−0.0086(17)	−0.2303(8)	0.0036(18)	2.10	2.13
O(5)	0.7265(11)	0.4950(18)	0.4033(8)	0.0049(19)	2.03	1.96
O(6)	0.4957(11)	0.0936(17)	0.2889(9)	0.0043(19)	2.15	2.06
O(7)	0.1258(11)	−0.3354(16)	−0.0996(9)	0.0036(19)	1.85	1.85
O(8)	0.7127(11)	0.2243(17)	0.2032(9)	0.0046(19)	2.27	2.10
O(9)	0.9447(12)	0.0829(18)	0.3639(9)	0.007(2)	2.04	1.99
O(10)	0.0905(11)	0.2347(18)	0.0762(9)	0.006(2)	2.05	2.05
B(1)	−0.1952(16)	−0.128(3)	−0.1585(13)	0.003(3)	3.04	3.04
B(2)	0.0079(16)	0.390(2)	0.1011(12)	0.002(3)	2.97	2.97
B(3)	0.3885(17)	0.202(3)	0.3286(13)	0.005(3)	2.93	2.93
B(4)	0.2176(17)	0.582(3)	−0.1728(14)	0.006(3)	2.98	2.98

[a]Calculated using bond-valence parameters from Brese and O'Keeffe [43] for all bonds.
[b]Calculated using bond-valence parameters for the Ba–O and B–O bonds from Brese and O'Keeffe [43] and for the Bi–O bonds from Krivovichev and Filatov [41].
[c]Fixed during refinement.

There is one symmetrically non-equivalent Ba site coordinated by twelve oxygen atoms in range of 2.747–3.192 Å with the average ⟨Ba–O⟩ bond length of 2.955 Å. The eight short bond lengths are distributed within the narrow interval of 2.747–2.909 Å with the average bond length of 2.813 Å (Table 3).

There are two Bi atoms in the structure and both are coordinated by seven O atoms (Fig. 2). As it can be seen from Table 3 and Fig. 2, both Bi atoms have irregular coordination polyhedra due to the stereoactivity of the $6s^2$ lone pair of electrons on Bi^{3+} cations [41,42]. Both $Bi(1)O_7$ and $Bi(2)O_7$ configurations are highly asymmetric with four short bonds (2.11–2.40 Å) complemented by three longer ones (2.59–3.13 Å). In the $Bi(1)O_7$ polyhedron, four short bond lengths vary from 2.114 to 2.398 Å with ⟨Bi–O⟩ = 2.255 Å, and the next neighboring oxygen atoms are more than 2.631 Å apart (Table 3). In the $Bi(2)O_7$ polyhedron, four short bond lengths are in the range of 2.138–2.374 Å with ⟨Bi–O⟩ = 2.256 Å and the next neighboring oxygen atoms are more than at 2.59 Å apart. The Bi(1) and Bi(2) polyhedra can be considered as BiO_4 distorted tetragonal pyramids formed by short Bi–O bonds (Figs. 2 and 3) with Bi atoms at the apices of the pyramids.

The O(1), O(2), O(4), O(7) and O(10) atoms are coordinated by two B atoms so that they are bridging ones in the borate anion (see below). The O(3), O(5), O(6), O(8) and O(9) atoms are terminal in the BO-polyhedra and they are bonded to one or two Bi atoms as well.

3.1.2. Bond-valence analysis

Bond-valence sums (BVS) for atoms in the structure of $BaBi_2B_4O_{10}$ are listed in Table 3. They were calculated using the bond-valence parameters for all bonds from [43], and also for the Ba–O and B–O bonds from [43] and for the Bi–O bonds ($r_o = 1.990$ Å, $b = 0.48$) taken from [42]. All bond-valence sums (Table 3) are in agreement with the expected values. From Table 3 we can see that coordination number equal to 8 is right for BaO polyhedron rather than 12.

3.1.3. Structure of the borate anion

In the structure of $BaBi_2B_4O_{10}$, the borate polyhedra share their corners to form a new $[B_4O_{10}]^{8-}_{\infty}$ chain that has not previously been observed in borates. A portion of the borate chain contained in the asymmetric unit is shown in Fig. 1. The borate anion can be described as consisting of two borate fundamental building blocks (FBB): a triborate group of three tetrahedra (B(1), B(3) and B(4) atoms) and the single BO_3 triangle (formed by the B(2) atom). According to modern descriptions of borate groups by Touboul et al. [44] and Burns et al. [40], the asymmetric unit is symbolized as $4B:\infty^1[(3{:}3T)+(1{:}\Delta)]$ or $\langle 3\square\rangle\Delta$, respectively, where 4B means four boron atoms composing the asymmetric unit and the BO_4 tetrahedron is denoted as T or γ, respectively, and the BO_3 triangle is denoted as Δ. The notation ∞^1 in Touboul's system means 1D-dimensionality of the borate anion. The symbol of the triborate group is $3{:}3T$ [44] or $3B:\langle 3\square\rangle$ [40], in the last notation the ⟨ ⟩ delimiters indicate that borate polyhedra form a ring. Similar rings of three tetrahedra occur in borate structures as an isolated group in nifontovite $Ca_2B_5O_3(OH)_2{*}2H_2O$ [45], as a part of isolated cluster in uralborite $Ca_2B_4O_4(OH)_8$ [46] and as a part of asymmetrical unit in the frameworks of low and high boracite $Mg_3B_7O_{13}Cl$ [47,48], etc.

Table 3
Selected bond lengths (Å) in the structure of $BaBi_2B_4O_{10}$

Bond	d (Å)	Bond valence[a]	Bond valence[b]
Bi(1)–O(3)	2.114(11)	0.94	0.77
Bi(1)–O(6)	2.171(10)	0.80	0.69
Bi(1)–O(8)	2.337(11)	0.51	0.49
Bi(1)–O(5)	2.398(11)	0.43	0.43
Bi(1)–O(3′)	2.631(11)	0.23	0.26
Bi(1)–O(2)	2.729(10)	0.18	0.21
Bi(1)–O(6′)	2.889(10)	0.12	0.15
$\langle$Bi(1)–O$\rangle_4/BVS$	2.255	2.68	2.38
$\langle$Bi(1)–O$\rangle_7/BVS$	2.467	3.21	3.00
Bi(2)–O(8)	2.138(10)	0.88	0.73
Bi(2)–O(5)	2.239(11)	0.67	0.60
Bi(2)–O(9)	2.272(11)	0.61	0.56
Bi(2)–O(6)	2.374(11)	0.46	0.45
Bi(2)–O(2)	2.590(11)	0.26	0.29
Bi(2)–O(2′)	2.900(10)	0.11	0.15
Bi(2)–O(4)	3.130(10)	0.06	0.09
$\langle$Bi(2)–O$\rangle_4/BVS$	2.256	2.62	2.34
$\langle$Bi(2)–O$\rangle_7/BVS$	2.520	3.05	2.86
Ba–O(4)	2.747(10)	0.29	
Ba–O(10)	2.748(11)	0.29	
Ba–O(9)	2.748(11)	0.29	
Ba–O(7)	2.753(10)	0.29	
Ba–O(1)	2.852(12)	0.22	
Ba–O(2)	2.863(10)	0.21	
Ba–O(5)	2.883(10)	0.20	
Ba–O(8)	2.909(11)	0.19	
Ba–O(3)	3.088(10)	0.12	
Ba–O(4′)	3.121(11)	0.11	
Ba–O(9′)	3.141(10)	0.10	
Ba–O(10′)	3.192(11)	0.09	
$\langle$Ba–O$\rangle_8/BVS$	2.813	1.98	
$\langle$Ba–O$\rangle_{12}/BVS$	2.955	2.39	
B(1)–O(4)	1.439(19)	0.83	
B(1)–O(10)	1.469(19)	0.77	
B(1)–O(5)	1.489(19)	0.73	
B(1)–O(2)	1.494(19)	0.72	
$\langle$B(1)–O$\rangle/BVS$	1.473	3.05	
B(2)–O(9)	1.356(19)	1.04	
B(2)–O(10)	1.374(19)	0.99	
B(2)–O(7)	1.396(18)	0.93	
$\langle$B(2)–O$\rangle/BVS$	1.375	2.97	
B(3)–O(3)	1.46(2)	0.79	
B(3)–O(6)	1.466(19)	0.77	
B(3)–O(1)	1.47(2)	0.77	
B(3)–O(2)	1.557(19)	0.60	
$\langle$B(3)–O$\rangle/BVS$	1.488	2.93	
B(4)–O(1)	1.43(2)	0.85	
B(4)–O(4)	1.449(19)	0.81	
B(4)–O(8)	1.51(2)	0.69	
B(4)–O(7)	1.54(2)	0.63	
$\langle$B(4)–O$\rangle/BVS$	1.482	2.98	

[a]Calculated using bond-valence parameters from Brese and O'Keeffe [43] for all bonds.
[b]Calculated using bond-valence parameters for the Ba-O and B-O bonds from Brese and O'Keeffe [43] and for the Bi-O bonds from Krivovichev and Filatov [41].

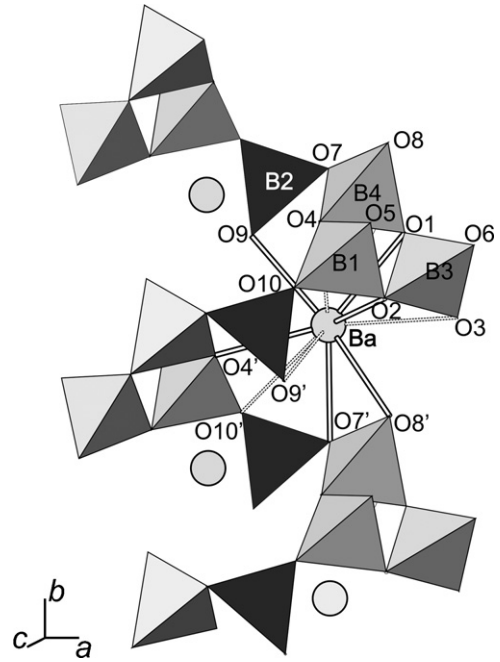

Fig. 1. The one-dimensional borate anion and coordination of the Ba^{2+} cation in the structure of $BaBi_2B_4O_{10}$ projected along the *b*-axis.

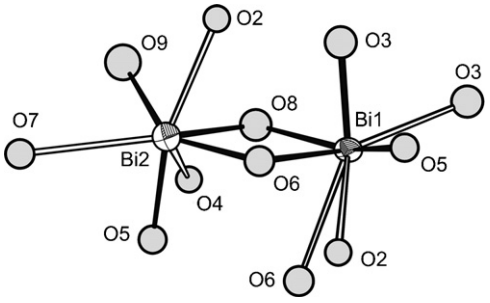

Fig. 2. The Bi_2O_{10} bismuthate group. Short and long bonds are shown as black and white lines, respectively.

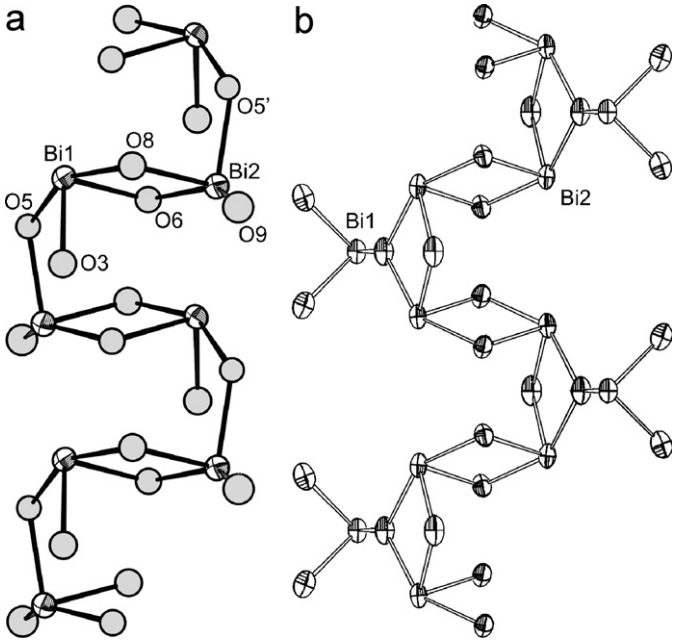

Fig. 3. The similar bismuthate anionic chains in (a) $BaBi_2B_4O_{10}$ and (b) $Bi_3B_5O_{12}$ structures shown in projection along the *b*-axis.

3.1.4. Bismuthate groups

Two distorted $Bi(1)O_7$ and $Bi(2)O_7$ polyhedra share a common edge O6–O8 to form $[Bi_2O_{10}]^{14-}$ groups (Fig. 2) the Bi(1)–Bi(2) bond length is equal to 3.56 Å in these groups. These double groups sharing a common edge are typical for the Bi oxocompounds. In Fig. 2 the Bi_2O_6 groups composed of BiO_4 distorted tetragonal pyramids formed by short Bi–O bonds are given in black color. Central atoms of both pyramids, Bi(1) and Bi(2), and two O atoms forming common O(6)–O(8) edge compose a rhomb (Figs. 2–4) in the *ac* monoclinic plane which is one of the strongest fragments of the structure. The Bi_2O_6 groups are connected via common O(5) atoms to form $[Bi_2O_5]^{4-}$ bismuthate chains extended along the *b*-axis (Fig. 3a). The Bi(1)–Bi(2) bond lengths in the chains are equal to 3.72 and 4.00 Å.The similar chains of BiO_4 pyramids with the Bi–Bi bond lengths equal to 3.57 and 3.60 Å (Fig. 3b) are formed in the crystal structure of $Bi_3B_5O_{12}$ [25].

3.1.5. Structure description

The structure of $BaBi_2B_4O_{10}$ is shown in Fig. 4a. It is based upon thick layers that are parallel to (001). Layers can be described as built from alternate spiral $[B_4O_{10}]^{8-}$ borate chains and the $[Bi_2O_5]^{4-}$ bismuthate chains. The short Bi–O bonds link Bi atoms to terminal O atoms of the BO_3 and BO_4 polyhedra from the borate chains. The borate chains are interleaved with rows of the Ba^{2+} cations along the *c*-axis so that the Ba atoms are located within the layers. The BaO_{12} polyhedra are condensed to form sheets parallel to (100) while the BaO_8 polyhedra formed by short Ba–O bonds are single ones they share common O(1)–O(2) and O(7)–O(8) edges with the $B(3)O_4$ and $B(4)O_4$ tetrahedra from the chains (Fig. 1) of the same layer and the O(5)–O(10) edges with the $B(1)O_4$ tetrahedra from adjacent layer (Fig. 4a). Thus the layers are connected by the Ba–O(5) and Ba–O(10) bonds with strength of the bonds equal to 0.20 and 0.29 v.u., respectively, as well as by two equivalent Bi(1)–O(3) bonds with strength of 0.23 v.u. each (Fig. 4a).

3.2. Thermal expansion of the crystal structure

The expansion of $BaBi_2B_4O_{10}$ in the range of 20–700 °C is highly anisotropic. Whereas the *b* and *c* unit-cell parameters increase on heating almost linearly, temperature dependencies of the *a* and *β* parameters undergo a flexion at ~200–300 °C (Fig. 5). Before this temperature,

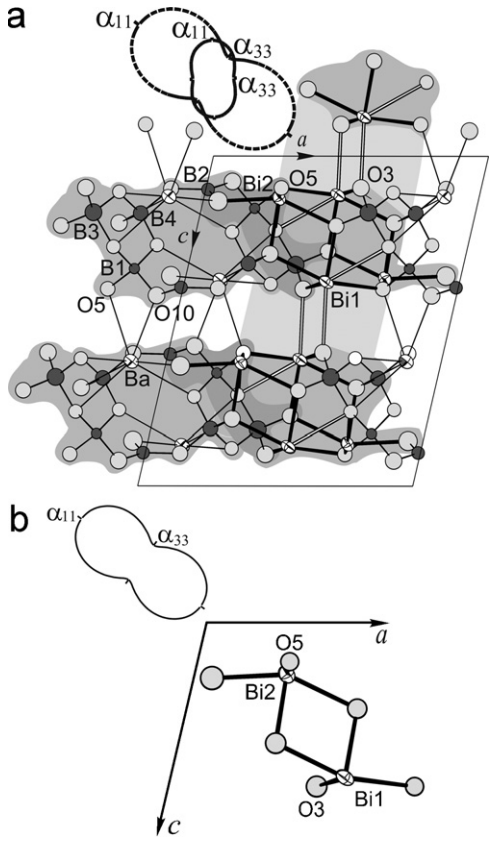

Fig. 4. The crystal structure of $BaBi_2B_4O_{10}$ and pole figures of the thermal expansion coefficients for 200 and 600 °C (continuous and dotted lines, respectively) within the *ac* monoclinic plane (a) and fragment showing the Bi–O hinge mechanism of the thermal expansion (b). The borate and bismuthate anionic chains and their superpositions forming layers are marked by light-gray, gray and dark-gray regions, respectively.

the *a* parameter increases very slowly, whereas, after 300 °C, it increases more drastically. The β angle first increases slightly that it is not so typical for monoclinic crystals [49], and, above 300 °C, decreases to prove the general tendency that the β angle tends to 90° in the direction of higher symmetry. Whereas temperature dependencies for the *b* and *c* parameters and the unit cell volume were approximated linearly, the behavior of *a* and β has been approximated by a quadratic polynom. Final approximation equations are

$$a(t) = 10.156(4) - 0.00002(3) \times t + 0.00000022(4) \times t^2,$$
$$b(t) = 6.371(1) + 0.000050(4) \times t,$$
$$c(t) = 12.475(2) + 0.000159(5) \times t,$$
$$\beta(t) = 102.76(2) + 0.00038(15) \times t - 0.0000012(2) \times t^2,$$
$$V(t) = 784.3(2) + 0.0309(6) \times t.$$

Main coefficients of thermal expansion tensor at different temperatures calculated using these equations are presented in the Table 4. In the monoclinic system, the α_{22} tensor axis is oriented towards the *b*-axis and the α_{11} and α_{33} axes are in the monoclinic plane forming the μ angle between the α_{33} and *c* axes. It can be seen (Table 4) that on heating the α_{11} and α_{33} coefficients increase from 13 and $-3 \times 10^{-6}\,°C^{-1}$ up to 37 and $9 \times 10^{-6}\,°C^{-1}$, respectively, while α_{22} remains practically constant at $11 \times 10^{-6}\,°C^{-1}$. On heating, the α_{11} and α_{33} axes change their directions as a consequence of quadratic polynomial temperature dependence of the *a* and β unit-cell parameters. Bulk thermal expansion increases more than twice on heating up to 700 °C that can be attributed to the increase in thermal mobility of Bi^{3+} and Ba^{2+} cations.

The thermal expansion coefficient figures are shown in Fig. 4 for lower (200 °C, solid line) and higher (600 °C, dotted line) temperatures. At the stage of initial heating (20–200 °C) the β angle slightly increases ($\alpha\beta = 2 \times 10^{-6}\,°C^{-1}$), and the structure expands most intensely along directions close to the *c*-axis perpendicular to the layers. This character of thermal expansion is typical for the layered structures. At higher temperatures (400–700 °C), a hinge mechanism of thermal deformations has been recognized [49]. The latter can be viewed as a deformation of the *ac* monoclinic plane due to the change in the β angle. Since, at higher temperatures, the β angle decreases with the increase in temperature ($\alpha\beta = -9 \times 10^{-6}\,°C^{-1}$), the structure expands intensely along the $\boldsymbol{a}+\boldsymbol{c}$ vector (short diagonal of the *ac* parallelogram) and less intensely along long diagonal (Fig. 4).

In other words, thermal deformations of the studied compound are very complex. There are two points that deserve attention: (1) change in the thermal behavior at ~200 °C; (2) synchronous change of the thermal expansion character for the α and β parameters. It can be suggested that the compound experiences hinge-type deformations at higher temperatures and these start at ~200 °C.

In order to understand thermal expansion of $BaBi_2B_4O_{10}$, we use the ideas suggested in [50] to explain thermal expansion of tenorite, CuO. Hinge transformations are characteristic for the part of the structure that has strong bonds linked at O atoms that can be considered as hinge points. As it was mentioned above, this is the case for the planar configuration of the 2Bi and 2O atoms (Fig. 4b), where the Bi atoms are separated by 3.56 Å that is higher than the sum of ionic radii of Bi^{3+} (3.20 Å). At lower temperatures, the two Bi atoms do not interact with each other. At higher temperatures, their thermal oscillations increase. Figs. 4a and b show that, even at room temperature, the Bi(1) and Bi(2) displacement ellipsoids are elongated towards each other. At higher temperatures, the Bi atoms experience repulsive interactions that makes the structure expanding along the $\boldsymbol{a}+\boldsymbol{c}$ vector. This results in the decrease of the β angle and expansion along the *a*-axis. The temperature of 200–300 °C when the Bi atoms start to interact can be called 'hinge-turn-on' temperature [51]. After CuO, the structure of $BaBi_2B_4O_{10}$ is yet another example of this kind of behavior.

4. Conclusion

In conclusion, we have been successful in preparation of single crystals of $BaBi_2B_4O_{10}$, a new compound in the

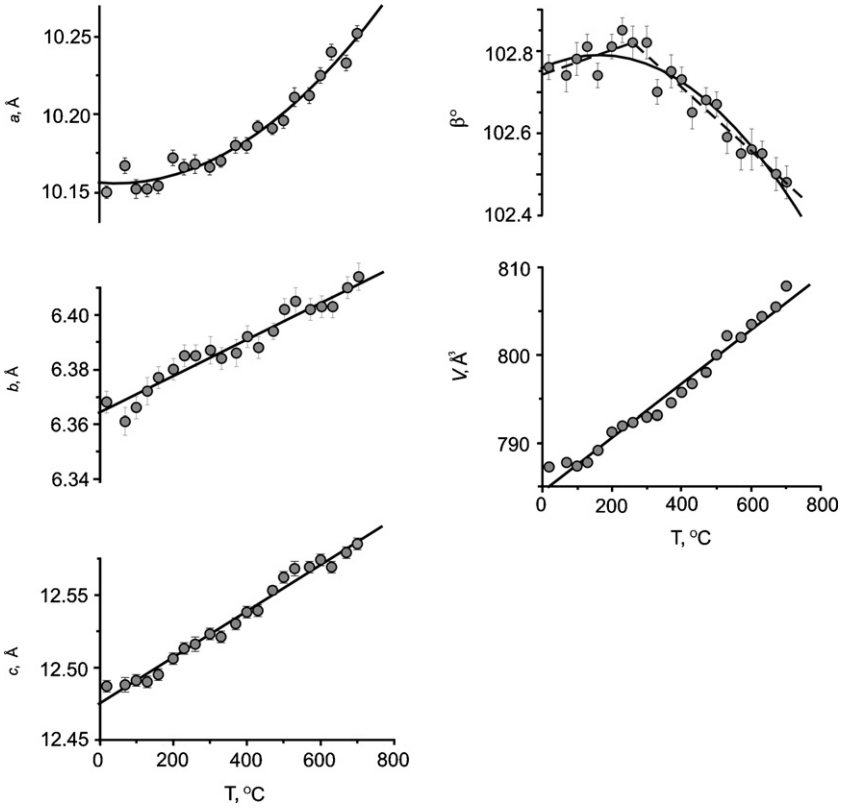

Fig. 5. Temperature dependencies of the unit-cell parameters and volume for $BaBi_2B_4O_{10}$.

Table 4
Main coefficients ($\times 10^6\,^{\circ}C^{-1}$) of thermal expansion tensor for $BaBi_2B_4O_{10}$

T, °C	α_{11}	α_{22}	α_{33}	μ[a]	$\langle\alpha\rangle$	α_v
20	13	11	−3	85	7	21
50	13	11	−1	86	8	23
100	13	11	2	89	9	26
150	13	11	4	86	9	28
200	13	11	7	76	10	31
250	14	11	8	62	11	33
300	15	11	9	47	12	35
350	18	11	10	37	13	39
400	20	11	10	31	14	41
450	23	11	10	28	15	44
500	26	11	10	25	16	47
550	28	11	10	24	16	49
600	31	11	9	23	17	51
650	34	11	9	22	18	54
700	37	11	9	21	19	57

[a] μ is the angle between the α_{33} and c axes; it is positive in the clockwise direction from c to α_{33} and negative otherwise.

$BaO–Bi_2O_3–B_2O_3$ system. Its structure solution demonstrated that it contains a novel type of chain borate anion, $[B_4O_{10}]^{8-}$, consisting of triborate rings of borate tetrahedra and single triangles. The compound belongs to a new structure type. Rigidity of the B–O and Bi–O bonds permit us to consider the new Ba–Bi borate as a barium 'borate-bismuthate'.

Thermal expansion of $BaBi_2B_4O_{10}$ is very complex. Above 200 °C highly anisotropic thermal oscillations of the Bi atoms and rigid Bi–O bonds result in highly anisotropic hinge mechanism of the thermal expansion.

Acknowledgments

This research has been supported by the Russian Foundation for Basic Research through Grants no. 05-03-33246 for R.S.B. and S.K.F., and through Grant

no. 05-03-32506 for A.V.E. and Yu.F.K. S.V.K. and S.K.F. thanks Russian Ministry of Science and Education for partial support (RNP 2.1.1.3077).

References

[1] T. Sasaki, Y. Mori, Y. Moshimura, Y.K. Yap, T. Kamimura, Mater. Sci. Eng. R. 30 (2000) 1–54.
[2] P. Egger, J. Hulliger, Coord. Chem. Rev. 183 (1999) 101–115.
[3] T. Sugawara, R. Komatsu, S. Uda, Solid. State Commun. 107 (1998) 233–237.
[4] M. Sheik-Bahae, M. Ebrahimzadeh, Opt. Commun. 142 (1997) 294–298.
[5] H.G. Giesber, J. Ballato, W.T. Pennington, J.W. Kolis, Information Sci. 149 (2003) 61–68.
[6] H.-R. Jung, B.-M. Jin, J.-W. Cha, J.-N. Kim, Matter. Lett. 30 (1997) 41–45.
[7] N.I. Leonyuk, E.V. Koporulina, V.V. Maltsev, O.V. Pilipenko, M.D. Melekhova, A.V. Mokhov, Optic. Mater. 26 (2004) 443–447.
[8] E.F. Dolzhenkova, A.N. Shekhovtsov, A.V. Tolmachev, M.F. Dubovik, B.V. Grinyov, V.A. Tarasov, V.N. Baumer, O.V. Zelenskaya, J. Cryst. Growth. 233 (2001) 473–476.
[9] Z. Lin, Z. Wang, C. Chen, M.H. Lee, J. Appl. Phys. 90 (2001) 5585–5588.
[10] D. Xue, K. Betzler, H. Hesse, D. Lammers, Solid State Commun. 114 (2000) 21–25.
[11] Yu.F. Kargin, A.V. Egorysheva, Russ. J. Inorg. Chem. 50 (2005) 1942–1946 [Translated from Zhurnal Neorganicheskoi Khimii. 50 (2005)].
[12] A.V. Egorysheva, Yu.F. Kargin, V.M. Skorikov, Russ. J. Inorg. Chem. 50 (2005) 1733–1736 [Translated from Zhurnal Neorganicheskoi Khimii. 50 (2005) 1851–1854].
[13] J. Barbier, N. Penin, A. Denoyer, L.M.D. Cranswick, Solid State Sci. 7 (2005) 1055–1061.
[14] A.V. Egorysheva, Yu.F. Kargin, V.M. Skorikov, Russ. J. Inorg. Chem. 51 (2006) 1106–1110 [Translated from Zhurnal Neorganicheskoi Khimii. 51 (2006) 1185–1189].
[15] A.V. Egorysheva, V.M. Skorikov, V.D. Volodin, O.E. Muslisky, Yu.F. Kargin, Russ J Inorg Chem 51 (2006) 1954–1960 [Translated from Zhurnal Neorganicheskoi Khimii. 51 (2006) 1185–1189].
[16] A.V. Egorysheva, Y.F. Kargin, Russ. J. Inorg. Chem 49 (2004) 470–474 [Translated from Zhurnal Neorganicheskoi Khimii. 49 (2004) 522–526].
[17] C.T. Chen, B.C. Wu, A.D. Jiang, G.M. You, Sci. Sin. B 28 (1985) 235.
[18] P.P. Fedorov, A.E. Kokh, N.G. Kononova, Russ. Chem. Rev. 71 (2002) 651–671.
[19] H. Hellwig, J. Liebertz, L. Bohaty, Solid State Commun. 109 (1999) 249–251.
[20] H. Hellwig, J. Liebertz, L. Bohaty, J. Appl. Phys. 88 (2000) 240–244.
[21] C. Du, Z. Wang, J. Liu, X. Xu, B. Teng, K. Fu, J. Wang, H. Jiang, Y. Liu, Z. Shao, Appl. Phys. B. 73 (2001) 215–217.
[22] M. Burianek, P. Held, M. Muhlberg, Cryst. Res. Technol. 37 (2002) 785–796.
[23] A. Hyman, A. Perloff, Acta Crystallogr. 28 (1972) 2007–2011.
[24] A. Vegas, F.H. Cano, S. Garcia-Blanco, J. Solid. State Chem. 17 (1976) 151–155.
[25] S.K. Filatov, Ju.F. Shepelev, R.S. Bubnova, N.A. Sennova, A.V. Egorysheva, Yu.F. Kargin, J. Solid State Chem. 177 (2004) 515–522.
[26] P. Becker, R. Frohlich, Z. Naturforsch. 59b (2004) 256–258.
[27] R. Frohlich, L. Bohaty, J. Liebertz, Acta Crystallogr. C 40 (1984) 343–344.
[28] L. Li, G. Li, Y. Wang, F. Liao, J. Lin, Inorg. Chem. 44 (2005) 8243–8248.
[29] B. Teng, W.T. Yu, J.Y. Wang, X.F. Cheng, S.M. Dong, Y.G. Liu, Acta Cryst. C 58 (2002) i25–i26.
[30] A.V. Egorysheva, A.S. Kanishcheva, Yu.F. Kargin, Yu.E. Gorbunova, Yu.N. Mikhailov, Russ. J. Inorg. Chem. 47 (2002) 1804–1808 [Translated from Zhurnal Neorganicheskoi Khimii. 47 (2002) 1961–1965].
[31] N.G. Furmanova, B.A. Maksimov, V.N. Molchanov, A.E. Kokh, N.G. Kononova, P.P. Fedorov, Crystallogrphr. Rep. 51 (2006) 219–225.
[32] A.D. Mighell, A. Perloff, S. Block, Acta Crystallogr. 20 (1966) 819–823.
[33] K. Marumo, F. Ohgaki, M. Tanaka, Research Laboratory on Engineering Materials, Tokyo Institute of Techmology: Report. 1990, pp. 1–11.
[34] S. Block, A. Perloff, Acta Crystallogr. 19 (1965) 297–300.
[35] J.L. Stone, D.A. Keszler, G. Aka, A. Kahn-Harari, T.A. Reynolds, Proc. SPIE 4268 (2001) 175–179.
[36] J. Krogh-Moe, M. Ihara, Acta Crystallogr. 25 (1969) 2153–2154.
[37] A. Altomare, G. Cascarano, C. Giacovazzo, A. Guagliardi, M.C. Burla, G. Polidori, M. Camalli, J. Appl. Crystallogr. 27 (1992) 435.
[38] G.M. Sheldrick, SHELXL-97, Program for the Refinement of Crystal Structures, Universität Göttingen, Germany, 1997.
[39] R. Belousov, S.K. Filatov, Glass Phys. Chem. (2007, in press).
[40] P.C. Burns, J.D. Grice, F.C. Hawthorne, Can. Miner. 22 (1995) 1131.
[41] S.V. Krivovichev, S.K. Filatov, Acta Crystallogr. B 55 (1999) 664–676.
[42] S.V. Krivovichev, S.K. Filatov, Crystal Chemistry of Minerals and Inorganic Compounds with Complexes of Anion Centered Tetrahedra, St.Petersburg State University, 2001 (in Russ.).
[43] N.E. Brese, M. O'Keeffe, Acta Crystallogr. B 47 (1991) 192–199.
[44] M. Touboul, N. Penin, G. Nowogrocki, Solid State Sci. 5 (2003) 1327–1342.
[45] M.A. Simonov, Y.K. Egorov-Tismenko, E.V. Kazanskaya, E.L. Belokoneva, N.V. Belov, Sov. Phys. Dokl. 23 (1978) 159–161.
[46] M.A. Simonov, Y.K. Egorov-Tismenko, N.V. Belov, Sov. Phys. Dokl. 22 (1977) 277–279.
[47] E. Dowty, J.R. Clark, Z. Krist. 138 (1973) 64–99.
[48] S. Sueno, J.R. Clark, J.J. Papike, J.A. Konnert, Amer. Miner. 58 (1973) 691–697.
[49] S.K. Filatov, R.M. Hazen, in: A.S. Marfunin (Ed.), Advanced Mineralogy, vol. 1, Springer, Berlin, 1994, pp. 76–90.
[50] M.I. Domnina, S.K. Filatov, I.I. Zuzukina, L.P. Vergasova, Inorg. Mater. 22 (1986) 1992 (in Russ.).
[51] S.K. Filatov, R.S. Bubnova (in press).